Admittance measurements of magnetic freezeout in n^--type GaAs

T. W. Hickmott
IBM Research Division, Thomas J. Watson Research Center, Yorktown Heights, New York 10598
(Received 26 May 1992)

Admittance measurements on an n^--type GaAs/$Al_xGa_{1-x}As$/n^+-type GaAs heterostructure (an $Al_xGa_{1-x}As$ capacitor) are used to study the dependence of the activation energy for ac transport, E_I, on magnetic field B. The capacitor studied has a substrate doping $N_S \sim 7\times10^{15}$ cm^{-3}, which is about one-half the doping for the metal-insulator transition in n-type GaAs. For $B \gtrsim 6$ T there is a magnetically induced Gray-Brown (GB) dip in capacitance-voltage curves at the flatband voltage. By analogy with thermal freezeout of donors or acceptors, the presence of a GB dip shows that magnetic freezeout occurs. Thermal admittance measurements at fixed bias, fixed magnetic field, and variable temperature and frequency show that E_I is proportional to magnetic field. An alternative method, magnetic admittance measurements at fixed bias, fixed temperature, and variable magnetic field and frequency, shows that energy can be expressed as $E_I = \alpha\mu_B B$, where μ_B is the Bohr magneton and α is temperature dependent. The measurements support a model in which an impurity band in n^--type GaAs is split into a lower energy band and a higher energy band.

INTRODUCTION

The Mott criterion for the metal-insulator transition, the transition from metallic conduction to activated conduction in a lightly doped, compensated, n-type semiconductor, is $(N_D^{1/3}a_H^*)\sim 0.25$, where N_D is the number of donors per cm^3 and a_H^* is the effective Bohr radius for electrons. For GaAs, $a_H^* = 9.8$ nm, and the metal-insulator transition occurs when $N_D \sim 1.6\times10^{16}$ cm$^{-3} = N_C$. For $N_D \sim 0.1N_C$, conduction is by carrier hopping, either by nearest-neighbor hopping or by variable-range hopping. For intermediate concentrations, when $N_C/4 \lesssim N_D \lesssim N_C$, the nature of conduction is still uncertain. In compensated semiconductors, electron-electron interaction can introduce a gap in the density of states at the Fermi level, the Coulomb gap. In uncompensated semiconductors, conduction is through impurity bands separated by the Hubbard gap. In the latter case the metal-insulator transition occurs when the upper and lower Hubbard bands overlap. The relative roles of disorder, of electron-electron interaction, and of correlated electron hopping in determining conduction when $N_C/4 \lesssim N_D \lesssim N_C$ are not yet fully understood.[1-3]

Magnetic fields provide a powerful tool for studying the metal-insulator transition in lightly doped semiconductors.[4] In a magnetic field B, the wave function of electrons on isolated donors shrinks in the direction perpendicular to B.[5] This causes a giant positive magnetoresistance, either due to magnetic localization of carriers or to magnetic freezeout of carriers. Magnetic localization decreases the probability of hopping conduction by decreasing the overlap of electron wave functions with nearby donor sites, thus decreasing the probability of an electron tunneling from a filled site to a neighboring empty donor.[6] Magnetic freezeout occurs when the cyclotron radius of an electron in a conduction band $L = (\hbar/eB)^{1/2}$ becomes comparable to the Bohr radius. For GaAs, magnetic freezeout occurs for $B \gtrsim 6.4$ T. Magnetic freezeout increases the energy separation between donors and the conduction band and reduces the concentration of carriers in a conduction band by localizing them close to positive donors, thus increasing the sample resistance. It also reduces the charge in the substrate due to ionized donors.

Capacitance measurements have been used to study hopping conduction in silicon[7,8] and in GaAs.[9-12] Recently, capacitance-voltage (C-V) and conductance-voltage (G-V) measurements on $Al_xGa_{1-x}As$ capacitors have been used to distinguish between magnetic localization and magnetic freezeout in lightly doped n-type GaAs.[13] An $Al_xGa_{1-x}As$ capacitor, shown schematically in Fig. 1(a), is grown by molecular-beam epitaxy (MBE) on an n^+-type GaAs wafer. It consists of an n^--type GaAs substrate of thickness d, an undoped $Al_xGa_{1-x}As$ layer of thickness w which is the dielectric of the $Al_xGa_{1-x}As$ capacitor, and an n^+-type GaAs layer which acts as a metallic gate. The substrate doping N_S is equal to $(N_D - N_A)$ where N_A is the number of acceptors per cm^3. In a magnetic field the resistance of the n^--type GaAs substrate increases exponentially with B; the temperature dependence of the substrate series resistance was used to determine ϵ_3, the activation energy for hopping conduction in the lightly doped substrate. Two samples were studied in detail. For sample A, $N_S \sim 1.7\times10^{15}$, and there was close agreement between experimental measurements and the percolation theory of hopping conduction in lightly doped semiconductors of Shklovskii and Efros, and of Ioselevich.[6,14] For sample B, $N_S \sim 7\times10^{15}$, the exponential increase in substrate resistance was due to magnetic freezeout of carriers, as evidenced by a magnetically induced Gray-Brown (GB) dip in capacitance of sample B at the flatband voltage V_{FB}.[15,16]

Admittance spectroscopy of semiconductor capacitors or diodes, in which one measures both the temperature and frequency dependence of capacitance and conduc-

tance, has been extensively used to measure semiconductor properties. Examples of the use of admittance spectroscopy include the measurement of the energies of deep levels in semiconductors,[17–19] the behavior of interface states in metal-oxide-semiconductor (MOS) capacitors,[20] the magnitude of heterostructure band offsets,[21] and the determination of activation energies for freezeout of shallow dopants in silicon or p-type GaAs.[22,23] In Ref. 23, evidence was found for impurity conduction in p-type GaAs when the number of acceptors was $N_A \sim 5\times10^{15}$ cm^{-3}, although the Mott criterion for the metal-insulator transition for heavy holes would require $N_A \sim 4\times10^{18}$ cm^{-3}.

In the present paper admittance measurements are used to measure the magnetic-field dependence of the activation energy for ac conduction in the n^--type GaAs layer of sample B of Ref. 13. They extend earlier measurements to higher fields, show that the activation energy depends on magnetic field, and provide a way to study conduction in samples that are on the insulator side of the metal-insulator transition. In addition, an alternative method, magnetic admittance spectroscopy, is introduced, in which admittance measurements are made at constant temperature and bias, but with varying magnetic field and frequency. The results give the dependence of an energy gap for ac conduction on magnetic field.

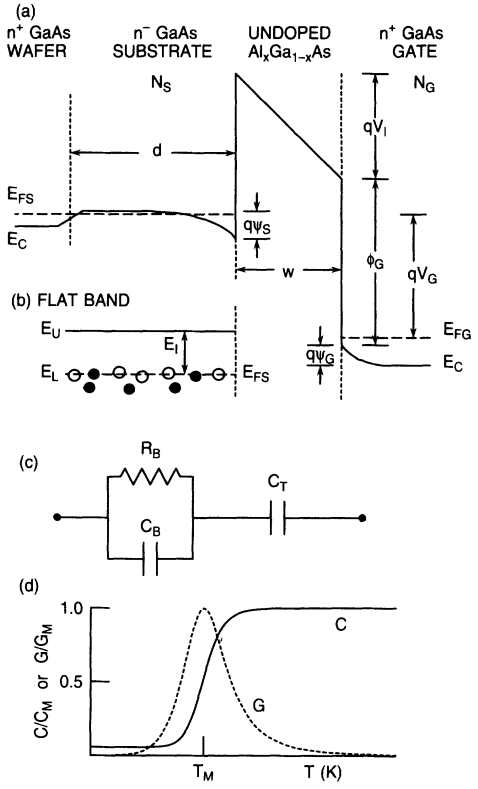

FIG. 1. (a) Schematic energy-band diagram for n^--type GaAs–$Al_xGa_{1-x}As$–n^+-type GaAs capacitor in accumulation. (b) Schematic energy-band diagram for carrier freezeout. (c) Equivalent circuit representation for impedance of an $Al_xGa_{1-x}As$ capacitor in accumulation. (d) Temperature dependence of parallel capacitance and conductance of the equivalent circuit of (c) calculated from Eqs. (2), (3), and (6).

EXPERIMENT

Figure 1(a) shows a schematic energy-band diagram of the n-type $Al_xGa_{1-x}As$ capacitor used to study magnetic freezeout in n^--type GaAs. The thickness of the undoped n^--type GaAs substrate d is ~1.0 μm; $N_S=(N_D-N_A)$ is $\sim7\times10^{15}$ cm^{-3}. The undoped $Al_{0.4}Ga_{0.6}As$ layer is 21.0 nm thick. The gate layer is ~300 nm thick; $N_G\sim1.8\times10^{18}$ cm^{-3}. The barrier height at the $Al_xGa_{1-x}As/n^+$-type GaAs interface is $\phi_G=0.263$ eV. The experimental methods to determine N_S, N_G, ϕ_G, d, and w are given in Ref. 13. The value of the compensation of the substrate, $K=N_A/N_D$, is not known but is estimated as $K\sim0.1$–0.3 from the MBE growth conditions and the background contamination of the MBE growth chamber. The sample area is 4.13×10^{-4} cm^2.

When a positive bias V_G is applied to the gate an electron accumulation layer forms on the n^--type GaAs substrate, as shown schematically in Fig. 1(a). The accumulation layer at the n^--type GaAs/$Al_xGa_{1-x}As$ interface is ~10–15 nm thick; it is less than 2% of the total thickness of the n^--type GaAs layer, ~1 μm. V_G divides into three parts; ψ_S is the band bending in the substrate, ψ_G is the band bending in the gate, and V_I is the voltage drop across the $Al_xGa_{1-x}As$ dielectric layer. If the substrate is in accumulation the equivalent circuit of Fig. 1(c) is an excellent representation. At constant V_G the capacitance

$$\frac{1}{C_T}=\frac{1}{C_S}+\frac{1}{C_I}+\frac{1}{C_G} \tag{1}$$

is nearly constant when temperature or magnetic field changes, where C_S, C_I, and C_G are the capacitances of the accumulated substrate, the $Al_xGa_{1-x}As$ dielectric and the gate, respectively. $C_I=\epsilon_I\epsilon_0A/w$, where ϵ_I is the dielectric constant of the $Al_xGa_{1-x}As$ insulator, ϵ_0 is the permittivity of free space, and A is the sample area. In a temperature or magnetic-field regime where the substrate freezes out, the lightly doped substrate is represented by a parallel resistance R_B and capacitance C_B. In accumulation C_S depends on V_G because of the dependence of the charge in the accumulation layer on V_G. R_B and C_B are determined by the thickness and dielectric constant of the bulk of the n^--type GaAs substrate. In the temperature or magnetic-field regime for freezeout, if one measures the admittance of the $Al_xGa_{1-x}As$ capacitor of Fig. 1(a) as a parallel capacitance C_P and a conductance G_P at an angular frequency $\omega=2\pi\nu$, where ν is the measurement frequency, then

$$\frac{C_P}{C_M}=\frac{1}{1+\omega^2(C_T+C_B)^2R_B^2}, \tag{2}$$

$$\frac{G_P}{G_M}=\frac{2\omega(C_T+C_B)R_B}{1+\omega^2(C_T+C_B)^2R_B^2}, \tag{3}$$

where G_M is the maximum value of conductance and $C_M=C_T$ is the maximum value of capacitance.[22,23] The Hewlett-Packard 4274A LCR meter used for capacitance

measurements measures G_P and C_P directly. The substrate capacitance is

$$C_B = \frac{\epsilon_S \epsilon_0 A}{d} , \tag{4}$$

where ϵ_S is the dielectric constant of GaAs and d is the thickness of lightly doped n^--type GaAs. If one defines a time

$$\tau_R = (C_T + C_B) R_B , \tag{5}$$

then G_P has a maximum and $C_P/C_M = 0.5$ when $\omega\tau_R = 1$. $(C_T + C_B)$ is essentially constant in the temperature range where freezeout occurs; only ϵ_S and ϵ_I depend on temperature and their change over the temperature range for freezeout is small. If the substrate freezes out, either due to temperature, magnetic field, or a combination of the two, the resistance can be expressed as

$$R_B = R_0 e^{E_I/kT} , \tag{6}$$

where R_0 is related to the resistance at high temperature, E_I is an ionization energy, and k is Boltzmann's constant. If Eq. (6) is valid, Eqs. (2) and (3) are equivalent to equations for Debye relaxation curves; they are plotted schematically in Fig. 1(d), as a function of temperature. By measuring the admittance of an $Al_xGa_{1-x}As$ capacitor as a function of temperature at different frequencies, a set of curves such as those of Fig. 1(d) is obtained, with T_M different for each frequency. E_I is determined from an Arrhenius plot of the logarithm of ω as a function of $1/T_M$. Even if Eq. (6) is not obeyed over the full temperature range to give an ideal Debye curve, at T_M, $\tau_R = 1/\omega$, and an activation energy can be determined.

Although measurements of parallel capacitance and conductance have been made with the LCR meter, the impedance of the capacitor can equally well be represented by an equivalent circuit of a capacitance C_S in series with a resistor R_S. C_S and R_S are obtained from G_P and C_P by the formulas

$$C_S = (1 + D^2) C_P , \tag{7}$$

$$R_S = \frac{D^2}{(1 + D^2) G_P} , \tag{8}$$

where

$$D = \frac{G_P}{\omega C_P} = \omega R_S C_S \tag{9}$$

is the dissipation factor. R_S depends primarily on the resistivity of the n^- GaAs layer. The temperature dependence of R_S was previously used to study localization and freezeout in n^--type GaAs.[13]

An experimental dependence of resistance of a semiconductor, such as in Eq. (6), which gives Debye-like admittance curves, is approximated by the thermal freezeout of carriers from a conduction (valence) band onto isolated donors (acceptors).[22,23] A generic model in which carriers can be excited from localized states across a mobility edge to a conduction band is shown in Fig. 1(b); E_L is the energy in the lower energy localized states, E_U is the energy in the extended states, and $E_I = (E_U - E_L)$ is the activation energy for the transition. This model corresponds to impurity conduction in the forbidden gap of a semiconductor as well as to excitation of donors to the conduction band or holes to the valence band.

The presence of localized states and a mobility edge, such as in Fig. 1(b), can introduce a characteristic GB dip in the capacitance of a semiconductor-insulator-semiconductor (SIS) capacitor at the flatband voltage V_{FB}.[13,15,16,23] In general, a GB dip occurs in C-V curves of a MOS or SIS capacitor when the majority carrier concentration in the lightly doped substrate is such that the Fermi level coincides with a donor (or acceptor) energy level in the semiconductor. Filling and emptying the impurity level at the ac measuring frequency produces an added capacitance that is in series with the insulator capacitance; the result is a dip in the total capacitance. Figure 2(a) shows a calculated C-V curve for an $Al_xGa_{1-x}As$ capacitor at 3.60 K with parameters that are similar to those for sample B.[24] Compensation is assumed to be $K = 0.1$. V_{SH} in Fig. 2(a) is the voltage by which the calculated C-V curves has been shifted so that V_{FB} coincides with V_{FB} of sample B, -0.045 V.[25] In Fig. 2(a), $E_I = 0.0001$ eV; Fig. 2(b) shows the region of the GB dip for different values of E_I, using an expanded voltage scale. Even with such a low value of E_I, there is a dip in the calculated C-V curve. The magnitude of the dip changes with energy but the voltage position is nearly constant. The behavior of an $Al_xGa_{1-x}As$ capacitor

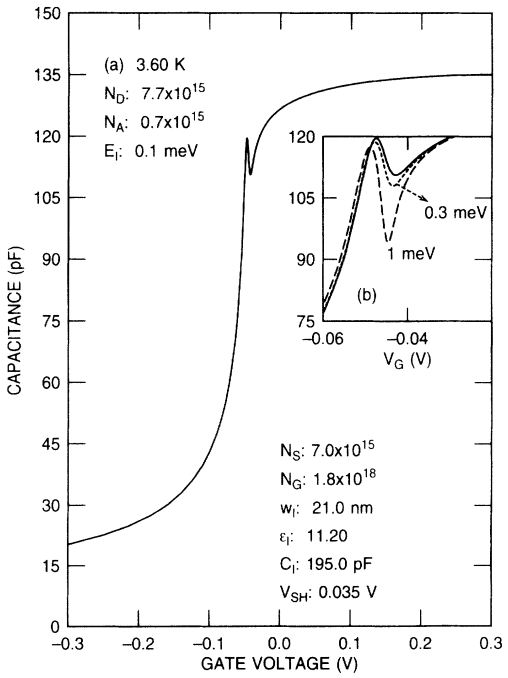

FIG. 2. (a) Capacitance-voltage curve at 3.60 K calculated from classical semiconductor-insulator-semiconductor model. Parameters approximate those of sample B. (b) Gray-Brown dip at V_{FB} of calculated C-V curve for different energies E_1, shown on an expanded voltage scale.

such as in Fig. 1(a) depends primarily on ψ_S. When $V_G < V_{FB}$, the substrate is in depletion and most of the applied voltage is across the lightly doped substrate. C_S in Eq. (1) becomes smaller and the total capacitance decreases. When $V_G > V_{FB}$, $\psi_S \cong \psi_G$ and most of V_G is dropped across the insulator, V_I. When $V_G = V_{FB}$, and if the Fermi level coincides with the energy of the localized states in the n^--type GaAs substrate, as shown schematically in Fig. 1(b), carriers are excited from E_L to E_U in phase with the ac voltage used to measure C_T; the result is an additional capacitance C_F, so that the total measured capacitance is

$$\frac{1}{C_T} = \frac{1}{C_S} + \frac{1}{C_I} + \frac{1}{C_G} + \frac{1}{C_F} . \tag{10}$$

The voltage range in which C_F is observed is narrow. A GB dip is generally observed as the temperature of a semiconductor is lowered.[23] At high temperatures the Fermi level E_{FS} is below E_L; at low temperatures E_{FS} is between E_L and E_U. A GB dip appears when E_{FS} and E_L approximately coincide. For a given E_I, the magnitude of the calculated GB dip increases as temperature decreases. Observation of a GB dip requires a change of charge in states at the substrate-dielectric interface.

Measurement procedures for C-V curves and admittance curves have been described previously.[13,23] For admittance measurements the $Al_xGa_{1-x}As$ capacitor was held at constant temperature, gate voltage, and magnetic field while frequency was varied. Seven frequencies between 1 and 100 kHz were used. The measurement voltage was then changed and the frequency cycle repeated. Typically, 14 to 16 voltages were measured at a given temperature and magnetic field. Unless otherwise noted, the magnetic field was parallel to the sample so there is no structure in C-V curves due to Landau levels in the accumulation region.[26] The sample was immersed in liquid helium during measurements. Temperatures between 1.5 and 4.1 K were measured and controlled by pumping on liquid He. The temperature interval between points of admittance curves is 0.03 K.

RESULTS

Figure 3 shows C-V and G-V curves at 10 kHz for sample B at 3.60 K and different parallel magnetic fields. The curves are typical of those at other temperatures, frequencies, and magnetic fields. They illustrate the characteristic features of magnetic freezeout that are the basis for admittance measurements. At 0 T, a depletion region forms in the substrate for $V_G \lesssim -0.05$ V and causes C to decrease. An accumulation layer forms for $V_G \gtrsim -0.05$ V, resulting in a nearly constant high capacitance for $V_G \gtrsim 0.0$ V. The exponential increase in G for $V_G \gtrsim 0.1$ V is due to electrons from the accumulation layer tunneling through the dielectric. The maximum voltage at which C-V and G-V curves can be measured is reached when the quality factor $Q = 1/D \sim 0.5$; for example, this occurs when $G = 1.9 \times 10^{-5}$ S for $\nu = 10$ kHz.

In a high magnetic field there is a dip in C at V_{FB}, as shown in Figs. 3(b)–3(d). This is a GB dip due to magnetic freezeout rather than to purely thermal freezeout of carriers. At 0 T there is an inflection at V_{FB} which is not well resolved. This may indicate a small amount of thermal freezeout of electrons, but the magnitude is not sufficient to produce a dip; a GB dip is only resolved for $B \gtrsim 6$ T and it occurs for all measurement frequencies. The decrease in maximum capacitance between 0.0 and 0.2 V at 11 and 14 T is due to increased series resistance of the substrate at higher magnetic fields. The decrease in capacitance for $V_G \gtrsim 0.2$ V at 11 and 14 T is due to depletion of carriers and band bending in the gate; it depends on N_G.

Independent confirmation that the GB dip occurs at V_{FB} is provided by measurement of current-voltage (I-V) and C-V curves when B is perpendicular to sample B. When $V_G > V_{FB}$ and B is perpendicular to the sample, a sequence of Landau levels forms in the two-dimensional gas of the accumulation layer on the substrate. As V_G increases, the number of electrons in the accumulation layer increases; electrons fill up successive Landau levels. Minima between Landau levels or between spin-split levels of a Landau level are reflected in minima in C-V, G-V, and I-V curves. Figure 4(a) shows C-V curves at 1.6 K, 10 kHz, and at 6 and 12 T for sample B. In both cases there is a GB dip at V_{FB}, just as in parallel magnetic field. In addition there are minima, labeled L_1 and L_2, due to completion of occupancy of Landau levels in the accumulation region of the substrate, and minima S_1 and S_2 due to spin splitting of Landau levels.[26,27] Values of B for S_1 and L_1 as a function of V_G are shown in Fig. 4(b). Their

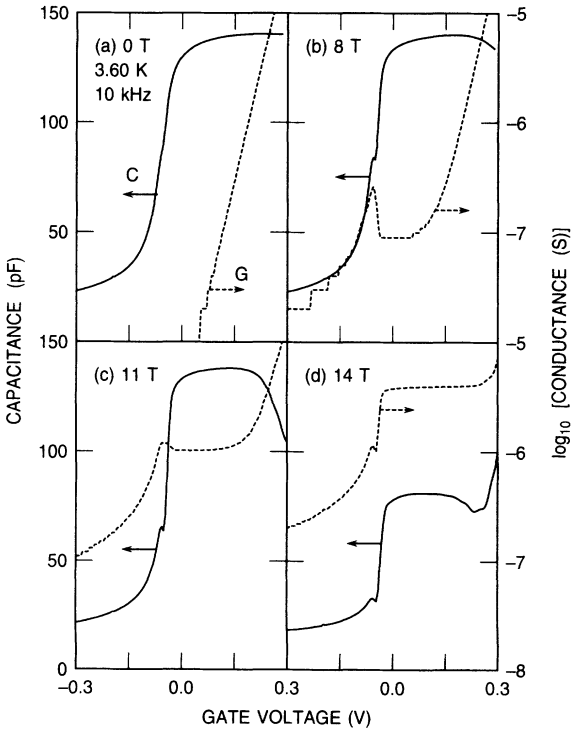

FIG. 3. Capacitance-voltage and conductance-voltage curves of sample B at 3.60 K, 10 kHz, and for different magnetic fields parallel to the sample.

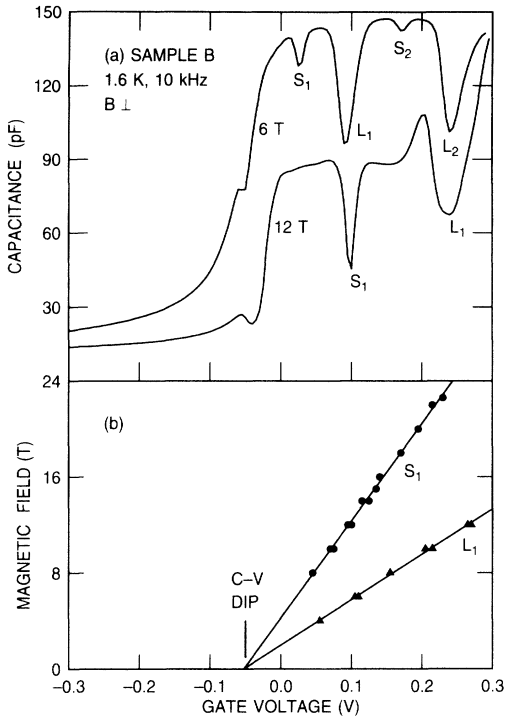

FIG. 4. (a) Capacitance-voltage curves for sample B at 1.6 K, 10 kHz, and different magnetic fields perpendicular to the sample. L_1 and L_2 indicate completion of filling of Landau levels; S_1 and S_2 indicate completion of filling of spin-split levels. (b) A fan diagram of the voltage for minima of C-V curves for sample B. Vertical line indicates voltage for Gray-Brown dip in C-V curve.

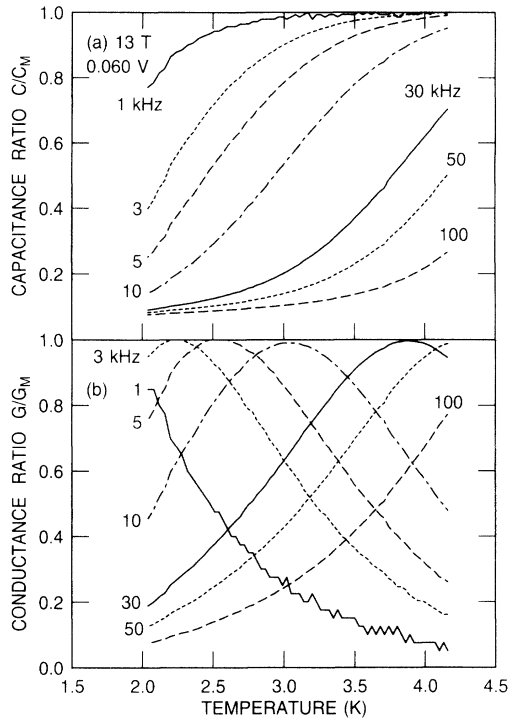

FIG. 5. Admittance plots for sample B at 13 T and $V_G = 0.060$ V. (a) C_P/C_M at different frequencies as a function of temperature. $C_M = 138$ pF. (b) G_P/G_M at different frequencies as a function of temperature. $G_M = 4.0\times10^{-7}$, 1.18×10^{-6}, 1.96×10^{-6}, 3.95×10^{-6}, 1.18×10^{-5}, 1.95×10^{-5}, and 3.87×10^{-5} S for $\nu = 1-100$ kHz.

extrapolation to $B=0$ defines V_{FB} and coincides with the GB dip in C-V curves. Values of V_G for minima in Fig. 4(b) are taken from both I-V and C-V curves; at high B substrate freezeout can shift the position of minima in C-V curves but has less effect on I-V curves.[28]

In Fig. 3(a), at 0 T, measurable ac conductance is due only to electron tunneling. As B increases there is an increase in conductance for V_G less than the voltage at which tunneling currents dominate G. There is a GB dip in G just as there is in C. There is a region of nearly constant G when $V_G > 0$ V; for $B \geq 9$ T this extends to $V_G = 0.2$ V. At constant temperature, as B increases, G in this region increases and then decreases as the resistance of the substrate becomes large. This is the voltage region in which admittance measurements are made.

Typical admittance curves for sample B are shown in Fig. 5. In Fig. 5(a), C/C_M is plotted as a function of temperature for different frequencies for $B=13$ T and $V_G = 0.060$ V; in Fig. 5(b), G/G_M is plotted. The particular value of V_G is chosen because it lies in the middle of the plateau region of conductance; other values of V_G would give similar results. C_M, the experimental maximum value of capacitance at each frequency, is taken from C-V curves at 0 T and the same V_G. G_M for each frequency is determined at some value of B and T where conductance curves have a maximum. G_M for any frequency is independent of B. The curves are nearly ideal Debye-like relaxation curves, as shown in Fig. 1(d). In Fig. 5(b), for 3 kHz $\leq \nu \leq$ 30 kHz, there is a maximum in G/G_M when $C/C_M = 0.5$. At higher frequencies the substrate resistance is high enough that $C/C_M < 0.5$ at all temperatures. Values of G_M are proportional to ω, in accord with Eq. (3).

Activation energies are obtained from admittance curves by plotting ω on a logarithmic scale as a function of $1/T_M$ where T_M is the temperature for the maximum in the curve of G/G_M at frequency ω for a given V_G and B. Figure 6 shows typical plots for different magnetic fields. For 10 T $\leq B \leq$ 14 T there are maxima in G/G_M for at least three frequencies; at 10 T, the frequencies are 100, 50, and 30 kHz; at 14 T they are 10, 5, and 3 kHz. For $B=9$ T there was a maximum in G/G_M at 100 kHz but not at lower frequencies so no energy is calculated. Solid lines are least-square fits of the data at the three highest frequencies; the activation energies are obtained from the slopes of the lines. Activation energies for V_G between 0.0 and 0.20 V are shown in Fig. 7 for different magnetic fields. The vertical lines are plus/minus the standard deviations of the least-square fits of the data at 10, 12, and 14 T. Within the accuracy of the data activation energies are proportional to B and independent of V_G at a given B. Values of energy from admittance curves are plotted in Fig. 9 as solid diamonds and labeled ω.

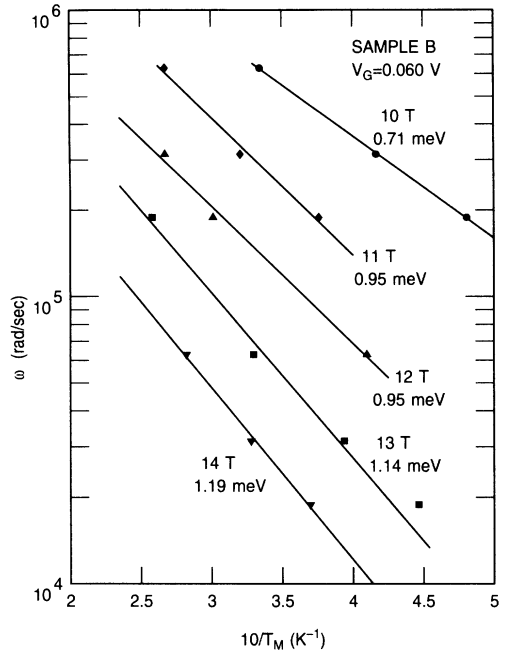

FIG. 6. Arrhenius plot of ω vs $1/T_M$ at constant V_G for different parallel magnetic fields. Activation energies use three highest frequency points.

An assumption in deriving activation energies from admittance curves is that Eq. (6) is obeyed, i.e., that the substrate resistance is an exponential function of E_I and $1/T$. Parallel capacitance and conductance of the $Al_xGa_{1-x}As$ capacitor are measured experimentally.

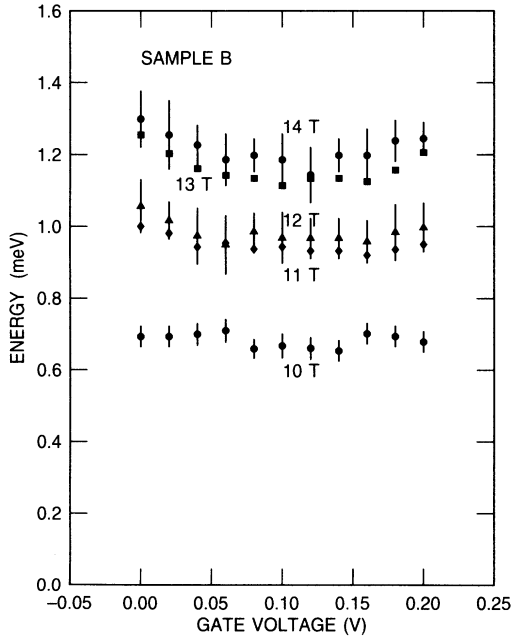

FIG. 7. Summary of measurements of the dependence of activation energy from admittance measurements on V_G in accumulation for different parallel magnetic fields. Vertical lines are plus/minus standard deviation of least-squares fit of data at 10, 12, and 14 T.

They may be converted to a series resistance and capacitance at each temperature by Eqs. (7)–(9); R_S depends primarily on substrate resistance. In Fig. 8 R_S is plotted on a logarithmic scale as a function of $1/T$ for measurements at 10 kHz, $V_G=0.060$ V, and different parallel magnetic fields. Each curve is shifted on the abscissa by one division. R_S is not a simple exponential function of $1/T$; in every case there is curvature in the plots. The solid lines are least-squares fits of the highest temperature points, between 4.1 and 3.0 K, for each of the values of B. Energies are higher than those from admittance measurements at the same value of B but, in both cases, are proportional to magnetic field. Values of energy determined from the temperature dependence of R_S are plotted as triangles in Fig. 9.

An alternate way of studying freezeout in $Al_xGa_{1-x}As$ capacitors is to use C-V-B or G-V-B curves in which one measures C and G at constant frequency while holding sample temperature and V_G constant and sweeping magnetic field. Figure 10 shows C-V-B and G-V-B curves at different frequencies for sample B at 1.7 K and $V_G=0.060$ V. The resemblance to the admittance curves of Fig. 1(d) or 5 is striking. In each case $G/G_M=1.0$ when $C/C_M=0.5$ and the peak in G/G_M shifts with changing frequency. However, magnetic field is the independent variable instead of temperature. Curves such as in Fig. 10 are magnetic admittance curves.

Analysis of admittance curves to obtain activation energies depends on an exponential relation between resistance and temperature such as in Eq. (6). The depen-

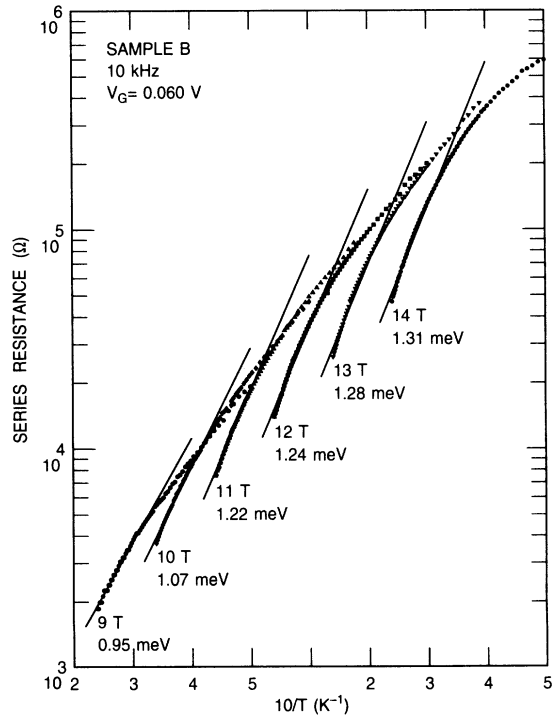

FIG. 8. Dependence of series resistance of n^--type GaAs at 10 kHz and $V_G=0.060$ V on $1/T$ for different magnetic fields. Solid lines are least-squares fit of highest temperature points. Curves are shifted on the abscissa by one division.

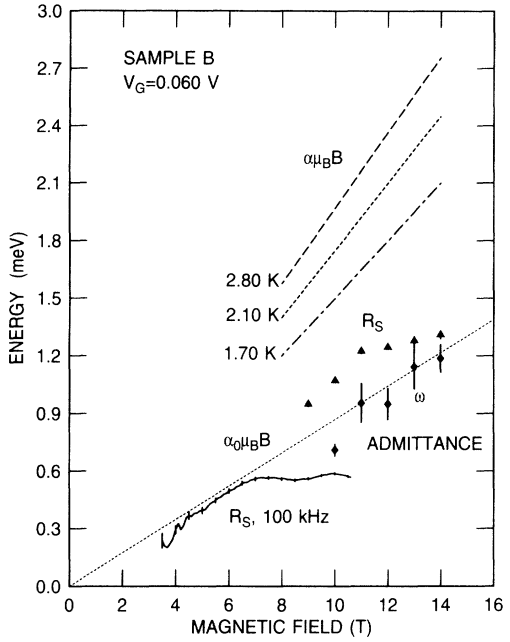

FIG. 9. Dependence of activation energy on magnetic field from thermal admittance data (points) and magnetic admittance data (lines).

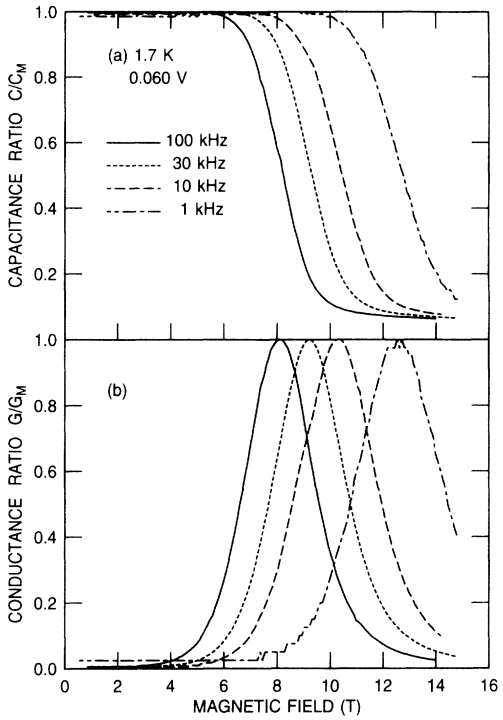

FIG. 10. Magnetic admittance plots for sample B at 1.7 K and $V_G = 0.060$ V. (a) C_P/C_M at different frequencies as a function of magnetic field. (b) G_P/G_M at different frequencies as a function of magnetic field.

dence of resistance on magnetic field can be expressed as

$$R_B = R_0 e^{\alpha\mu_B B/kT}, \tag{11}$$

where μ_B is the Bohr magneton and α is a constant. C-V-B and G-V-B curves such as in Fig. 10 can be converted to curves of series resistance versus magnetic field. Such curves are shown in Fig. 11 where R_S at 100 kHz and 0.060 V is plotted as a function of B for different temperatures. The exponential dependence of R_S on B holds reasonably well although there is curvature at higher values of B. Similar curves are obtained for measurements at 1 kHz $\leq \nu \leq$ 100 kHz.

Values of α in Eq. (11) are obtained from magnetic admittance curves by plotting ω on a logarithmic scale as a function of the magnetic field at the peak of G/G_M, B_M. Figure 12 shows such logarithmic plots for $V_G = 0.060$ V and three different temperatures. The lines are least-squares fits of the three highest frequency points; the lowest frequency point, $\nu = 1$ kHz, is less accurate than higher frequency measurements, and T_M cannot be determined at 2.8 K and 1 kHz. Figure 13(a) shows values of α for different values of V_G at three different temperatures. Vertical lines are plus/minus the standard deviation of the least-squares fit to the data. Within experimental uncertainty α is constant at a given temperature but is proportional to temperature, as shown in Fig. 13(b). The values of α are similar to values that Pepper found for the dependence of activation energy for conduction in an impurity band of GaAs on B;[29] he also discusses possible spin-related mechanisms for a magnetic-field dependence of activation energy. α is larger than the g value of electrons in GaAs, -0.44, by about a factor of 5. Whether α depends on spin-flip pro-

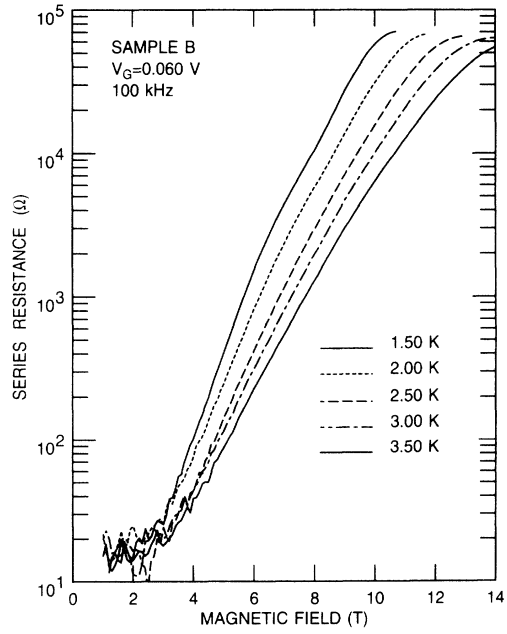

FIG. 11. Dependence of series resistance of n^--type GaAs at 100 kHz and $V_G = 0.060$ V on magnetic field at different temperatures for sample B.

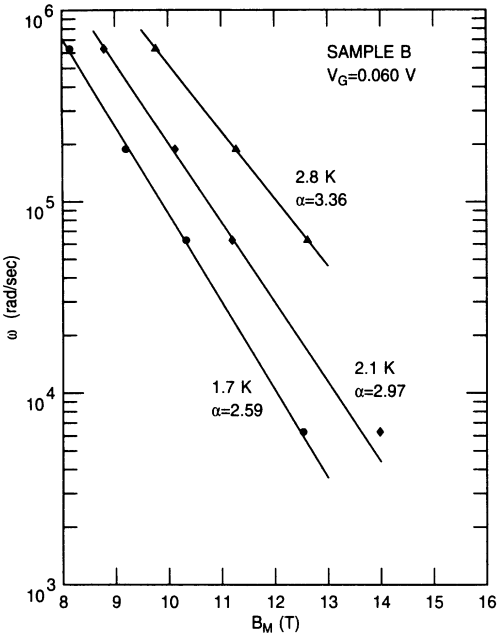

FIG. 12. Arrhenius plot of ω vs B_M at constant V_G for different temperatures. Activation energies use three highest frequency points.

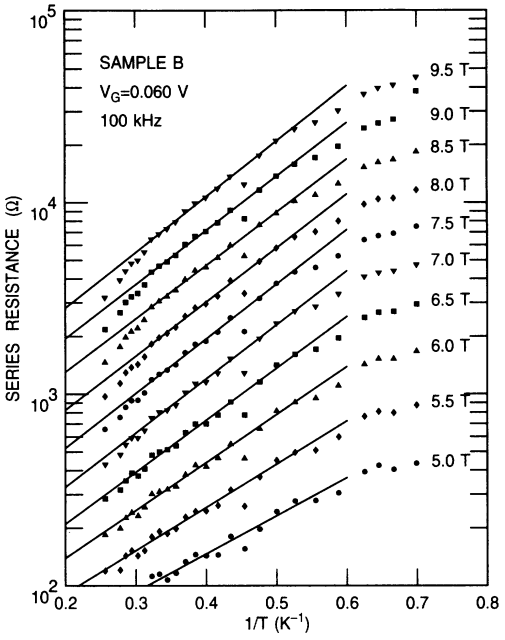

FIG. 14. Dependence of R_S at 100 kHz of n^--type GaAs on $1/T$ at different values of B for sample B. Solid lines are least-squares fit of data for $0.3 \leq 1/T \leq 0.5$ K^{-1}.

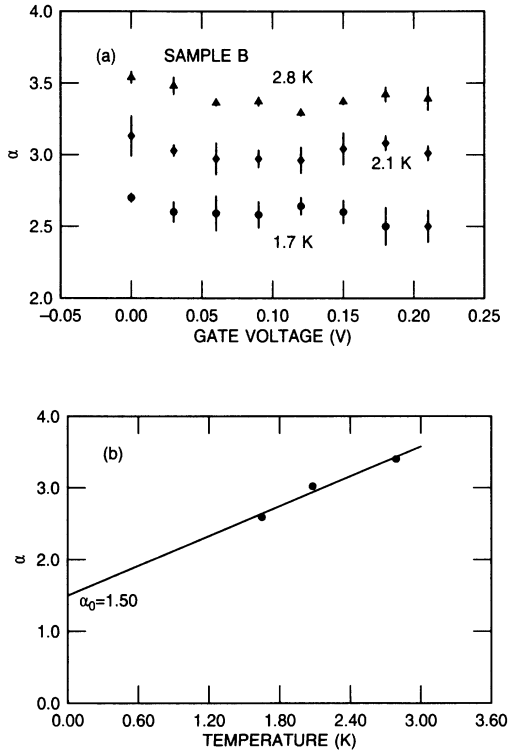

FIG. 13. (a) Dependence of α from magnetic admittance measurements on V_G in accumulation for different temperatures. Vertical lines are plus/minus standard deviation of least-squares fit of data. (b) Dependence of average value of α on temperature.

cesses of isolated donors is not clear. The three lines labeled with temperature in Fig. 9 are values of $\alpha\mu_B B$ obtained using the average values of α in Fig. 13(b). The lightly dotted line is $\alpha_0\mu_B B$ for $\alpha_0 = 1.50$, the extrapolated value of α at $T=0$ in Fig. 13(b).

To measure E_I from the temperature dependence of R_S, C-V-B and G-V-B curves such as those in Fig. 10 were measured at 100 kHz and 24 temperatures between 1.4 and 3.9 K, and the curves were converted to curves of R_S versus B, as in Fig. 11.[13] In Fig. 14, R_S is plotted on a logarithmic scale as a function of $1/T$ at different values of B. Activation energies are thus obtained as a function of B, and are plotted as the solid line in Fig. 9. Data between 2 and 3 K have been used for activation energies as shown by the solid lines in Fig. 14. At lower temperatures R_S is nearly constant with temperature, with some scatter in the data. The vertical lines every 0.5 T in Fig. 9 show the standard deviation of the least-squares fit of the data. The preexponential factor is proportional to B. No data are obtained below $\sim$3.5 T since, as shown in Fig. 11, R_S is too small to measure accurately. Data are not given above 10 T since the series resistance due to freezeout is large enough that meaningful data are not obtained at 100 kHz. Combining results from different methods of data analysis, there is a range of values of activation energy, as summarized in Fig. 9, but all the measurement methods show a dependence of energy on both magnetic field and on temperature.

DISCUSSION

The conventional method of measuring the temperature dependence of resistivity of semiconductors has been

dc conductance measurements of resistance and Hall effect.[1-3] The resistivity can be expressed as

$$\rho=\rho_1 e^{\epsilon_1/kT}+\rho_2 e^{\epsilon_2/kT}+\rho_3 e^{\epsilon_3/kT}, \quad (12)$$

where ϵ_1, ϵ_2, and ϵ_3 are activation energies for conduction in different temperature regimes. The different regimes are identified from plots of the logarithm of resistance versus $1/T$. ϵ_1 is the activation energy for freezeout of carriers from the conduction band onto ionized donors; for n-type GaAs, ϵ_1 is 5–6 meV. ϵ_2 is generally identified as the activation energy for carriers from the ground impurity state, the lower Hubbard band, to the band of doubly occupied impurity states, the upper Hubbard band. ϵ_3 is the activation energy for hopping conduction in the lower Hubbard band. In general, ϵ_2 conduction is not observed in plots of resistance versus $1/T$ for n-type GaAs. There is an extensive literature on experimental and theoretical aspects of ϵ_3 conduction.[1] $\epsilon_3 \sim 0.5$ meV for n-type GaAs with $(N_D-N_A) \lesssim N_C/2$; it decreases to 0 at the metal-insulator transition.[30]

The principal observation from C-V curves that cannot be made by other methods is the occurrence of a GB dip at the flatband voltage in the presence of a magnetic field. This shows that there is a change of charge in the n-type GaAs substrate that is in phase with the ac signal used to measure the sample admittance, as in the simplified model of Fig. 1(b). The large positive magnetoresistance of Fig. 8 or 11 is due to freezeout of electrons onto ionized donors as the magnetic field reduces the cyclotron radius of electrons to a magnitude comparable to the donors' Bohr radius. By analogy with thermal freezeout, such magnetic freezeout reduces the number of carriers that contribute to conduction through a band separated from the Fermi level, which is at approximately the same energy as isolated donors.

The alternate explanation for a large positive magnetoresistance applies to nearest-neighbor hopping. Hopping conduction depends on the tunneling of carriers from one site to another which depends, in turn, on the overlap of the wave functions of electrons on isolated donors. Large magnetic fields shrink the electron wave function, reduce the overlap, and thus reduce hopping conduction. As shown schematically in Fig. 1(b), nearest-neighbor hopping does not change the charge in a small region of the lightly doped semiconductor, and therefore no GB dip should be observed with increasing B. No GB dip has been observed for samples with $N_S \lesssim 3\times10^{15}$ cm^{-3}; only the present sample with $N_S \sim (7-8)\times10^{15}$ cm^{-3} has shown a GB dip due to magnetic freezeout.

The values of energy in Fig. 9 that are derived from plots of R_S at 100 kHz versus $1/T$ are comparable to values of ϵ_3 derived from dc resistivity measurements on Hall bars. For $B \lesssim 7$ T, energy is proportional to B. The values for $B \gtrsim 7$ T are nearly constant; the increase in R_S at higher B comes primarily from an increase in ρ_3, the preexponential term in Eq. (12), as shown in Fig. 14. However, for $B \gtrsim 7$ T, there is more curvature in plots of R_S versus $1/T$ than there is at lower B, which makes calculation of energy less accurate. If the higher temperature points were used, energies would be greater when $B \gtrsim 7$ T; calculated energies depend on the temperature range used for calculation. In general, energy values derived from temperature dependence of resistance are less than those derived from optical measurements, which give the most accurate values of trap depths and donor energies.[31] There is also a question as to whether temperature-dependent experiments give E_I or $E_I/2$, for example, in measuring donor or acceptor energies. For shallow donors and acceptors in semiconductors, whether one measures E_I or $E_1/2$ depends on compensation.[32] It is not clear whether there is a similar problem in determining energies for ϵ_3 processes.

Admittance measurements in a semiconductor depend on the modification of capture and emission rates of traps or impurities, which in turn changes the charge in a region of the semiconductor. They have been most frequently used to measure capture cross sections and energies of deep traps,[17-19] but have also been used to measure the properties of shallow impurities and interface states.[20-23] Temperature is the most common method of modifying emission states, but optical admittance measurements have been made in which changes of photon energy change the emission rate of traps.[19] The magnetic admittance curves of Fig. 10 are another example of the modification of the rate of change of charge emission by an external agent, the magnetic field.

Admittance measurements, when they can be done, require fewer assumptions about the detailed exponential dependence of resistance on temperature than Arrhenius plots such as those of Fig. 14. They depend on knowing ω, which is accurately known, and T_M. The occurrence of a GB dip at V_{FB} in high magnetic fields shows that there is a change of charge in the n^--type GaAs substrate due to emission and capture of carriers, which is the appropriate condition for applying admittance measurements. Activation energies from admittance measurements can be made for $B > 10$ T. The values are higher than from measurements of the temperature dependence of R_S at 100 kHz. Values of $\alpha\mu_B B$ at different temperatures are still higher. However, the lightly dotted line in Fig. 9, drawn for the value of α extrapolated to $T=0$, $\alpha_0=1.50$, is close to the experimental values of energy for the whole range of values of magnetic field. Thus measured energies depend on both temperature and magnetic field.

One of the continuing problems in understanding ϵ_3 processes for impurity conduction in lightly doped semiconductors is explaining why measured energies are not larger. According to Shklovskii and Efros,[33]

$$\epsilon_3=\frac{0.99e^2N_S^{1/3}}{4\pi\epsilon_S\epsilon_0}. \quad (13)$$

This implies that ϵ_3 should be higher for larger values of N_S. For $N_S=7\times10^{15}$, Eq. (13) predicts that $\epsilon_3=2.2$ meV. Experimentally $\epsilon_3 \sim 0.5$ meV for a wide range of N_S, decreasing to $\epsilon_3=0$ at the metal-insulator transition.[30] Equation (13) is derived on the assumption that conduction is by nearest-neighbor hopping. If there is an energy gap between the Fermi level and the states

through which conduction occurs, as appears to be the case for sample B, the assumption that nearest-neighbor hopping occurs may not be correct.

Two kinds of energy gaps have been proposed in lightly doped semiconductors; one is the gap between the lower Hubbard band and the upper Hubbard band in impurity conduction, the other is a Coulomb gap due to electron-electron interaction. The Coulomb gap occurs in the conduction regime when variable-range hopping (VRH) is important. The usual way to identify the occurrence of VRH is to plot resistivity versus $T^{-1/2}$ or $T^{-1/4}$ since $\rho \sim \exp(T_0/T)^x$ with $x=\frac{1}{4}$ if there is a constant density of states at the Fermi level and $x=\frac{1}{2}$ if there is a Coulomb gap and the density of states at the Fermi level goes to zero. Both $x=\frac{1}{2}$ and $\frac{1}{4}$ have been reported for conduction in GaAs; Mansfield summarizes the experimental data.[34] Neither plots of the logarithm of R_S versus $T^{-1/2}$ nor $T^{-1/4}$, using the data of Fig. 14, are linear so VRH cannot be unambiguously identified in sample B. However, the flattening out of the data at low temperature in Fig. 14 is suggestive of a transition from nearest-neighbor hopping to variable-range hopping.

Recently, both optical and electrical measurements have shown the occurrence of two bands within an impurity band which is split off from the conduction band in n-type GaAs.[35–37] Samples studied had doping between 1.3×10^{16} and 5.6×10^{16} cm^{-3}, i.e., on both sides of the critical concentration for the metal-insulator transition, $N_C=1.6\times10^{16}$ cm^{-3}. Sample B has $N_S=7-8\times10^{15}$ cm^{-3}. Observations of a GB dip in C-V curves are consistent with Drew's results and show that there is a splitting of the impurity band into two bands at $N_S \sim N_C/2$ as well as at concentrations greater than N_C.

In summary, C-V curves on an $Al_xGa_{1-x}As$ capacitor with $N_S \sim N_C/2$ show the existence of two bands in impurity conduction in n^--type GaAs. The critical concentration for the occurrence of two bands is between $N_S=3\times10^{15}$ and 7×10^{15} cm^{-3}. Activation energies determined by admittance measurements extend the measurements of energies determined from the dependence of the ac series resistance of n^--type GaAs on temperature to higher magnetic fields. An alternative technique, magnetic admittance curves, shows that the splitting between the upper and lower impurity bands depends on both magnetic field and temperature. The value of α_0, the proportionality constant for $E_I=\alpha\mu_B B$, is 1.5 at $T=0$. This suggests that spin-flip processes occur, but the origin of the splitting is unknown.

ACKNOWLEDGMENTS

It is a pleasure to acknowledge the help of S. L. Wright who grew the sample, and F. F. Fang who made the superconducting magnet available. I have benefited from many discussions with F. Stern who also provided critical comments on the manuscript.

[1] B. I Shklovskii and A. L Efros, *Electronic Properties of Doped Semiconductors* (Springer-Verlag, Berlin, 1984).
[2] J. A. Chroboczek, in *Noncrystalline Semiconductors, Vol. III,* edited by M. Pollak (CRC, Boca Raton, FL, 1987), p. 109.
[3] T. G. Castner, in *Hopping Transport in Solids,* edited by M. Pollak and B. I Shklovskii (North-Holland, Amsterdam, 1991), p. 1.
[4] M. Pepper, J. Non-Cryst. Solids **32**, 161 (1979).
[5] Y. Yafet, R. W. Keyes, and E. N. Adams, J. Phys. Chem. Solids **1**, 137 (1956).
[6] B. I. Shklovskii and A. L. Efros, *Electronic Properties of Doped Semiconductors* (Ref. 1), Chap. 7.
[7] T. G. Castner, Philos. Mag. B **42**, 873 (1980).
[8] T. G. Castner, W. N. Shafarman, and D. Koon, Philos. Mag. B **56**, 805 (1986).
[9] D. Redfield, Adv. Phys. **24**, 463 (1975).
[10] L. Eaves, P. S. S. Guimaraes, P. C. Main, I. P. Roche, J. A. Chroboczek, H. Mitter, J. C. Portal, and G. Hill, J. Phys. C **17**, L345 (1984).
[11] J. A. Chroboczek, L. Eaves, P. S. S. Guimaraes, P. C. Main, I. P Roche, H. Mitter, J. C. Portal, P. N. Butcher, M. Ketkar, and S. Summerfield, in *Proceedings of Seventeenth International Conference on Semiconductors,* edited by J. D. Chadi and W. A. Harrison (Springer-Verlag, New York, 1985), p. 697.
[12] R. Buczko, J. A. Chroboczek, and G. Wunner, Philos. Mag. Lett. **56**, 251 (1987).
[13] T. W. Hickmott, Phys. Rev. B **38**, 12 404 (1988).
[14] A. S. Ioselevich, Fiz. Tekh. Poluprovodn. **15**, 2373 (1981) [Sov. Phys.—Semicond. **15**, 1378 (1981)].
[15] P. V. Gray and D. M. Brown, Appl. Phys. Lett. **13**, 247 (1968).
[16] C. T. Sah, Solid State Electronics Laboratory Technical Report No. 1, Electrical Engineering Laboratory, University of Illinois, 1964, p. 62.
[17] D. L. Losee, J. Appl. Phys. **46**, 2204 (1975).
[18] J. L. Pautrat, B. Katircioglu, N. Magnea, D. Bensahel, J. C. Pfister, and L. Revoil, Solid State Electron. **23**, 1159 (1980).
[19] J. Barbolla, S. Duenas, and L. Bailón, Solid State Electron. **35**, 285 (1992).
[20] J. Shewchun, V. Temple, and R. Clarke, J. Appl. Phys. **43**, 3487 (1972).
[21] D. V. Lang, M, B. Panish, F. Capasso, J. Allam, R. A Hamm, A. M. Sergent, and W. T. Tsang, Appl. Phys. Lett. **50**, 736 (1987).
[22] S. Aymeloglu and J. N. Zemel, IEEE Trans. Electron. Dev. **ED-23**, 466 (1976).
[23] T. W. Hickmott, Phys. Rev. B **44**, 13 487 (1991).
[24] C-V curves at low temperature were calculated with a computer program provided by F. Stern. It is a continuum model that includes no quantum effects.
[25] T. W. Hickmott, P. M. Solomon, R. Fischer, and H. Morkoç, J. Appl. Phys. **57**, 2844 (1985).
[26] T. W. Hickmott, Phys. Rev. B **32**, 6531 (1985).
[27] T. W. Hickmott, Phys. Rev. B **39**, 5198 (1989).
[28] T. W. Hickmott, Phys. Rev. Lett. **57**, 751 (1986).
[29] M. Pepper, Philos. Mag. B **37**, 187 (1978).
[30] O. V. Emel'yanenko, T. S. Lagunova, D. N. Nasledov, D. D. Nedeoglo, and I. N. Timchenko, Fiz. Tekh. Poluprovodn. **7**, 1919 (1973) [Sov. Phys.—Semicond. **7**, 1280 (1974)].
[31] G. F. Neumark, Phys. Rev. B **5**, 408 (1972).

[32]J. S. Blakemore, *Semiconductor Statistics* (Macmillan, New York, 1962), p. 130.
[33]B. I. Shklovskii and A. L. Efros, *Electronic Properties of Doped Semiconductors* (Ref. 1), Chap. 8.
[34]R. Mansfield, in *Hopping Transport in Solids,* edited by M. Pollak and B. I. Shklovskii (North-Holland, Amsterdam, 1991), p. 349.
[35]M.-W. Lee, D. Romero, H. D. Drew, M. Shayegan, and B. S. Elman, Solid State Commun. **66**, 23 (1988).
[36]D. Romero, S. Liu, H. D. Drew, and K. Ploog, Phys. Rev. B **42**, 3179 (1990).
[37]S. Liu, H. Drew, A. Illiades, and S. Hadjipanteli, Phys. Rev. B **45**, 1155 (1992).